Pergamon

Journal of Structural Geology, Vol. 19, No. 9, pp. 1201 to 1217, 1997

0191-8141/97 $17.00 + 0.00

PII: S0191-8141(97)00034-5

Lateral extrusion in transpression zones: the importance of boundary conditions

RICHARD R. JONES

Østfold Research Foundation, Postboks 573, Halden 1754, Norway

and

ROBERT E. HOLDSWORTH and WAYNE BAILEY*

Department of Geological Sciences, University of Durham, Durham DH1 3LE, U.K.

(*Received* 23 *August* 1996; *accepted in revised form* 19 *March* 1997)

Abstract—The homogeneous transpression strain model formulated by Sanderson and Marchini (*Journal of Structural Geology* **6**, 449–458, 1984) has proved to be a useful tool in the analysis of complex three-dimensional deformation patterns. However, some of the boundary conditions introduced in the mathematical model may be unrealistic and unnecessarily restrictive. In this paper a strain matrix for unconfined transpression and transtension is derived in which material is allowed to move not only vertically, but also horizontally in and out of the deforming zone parallel to its length—'lateral extrusion'. Three end-member plane-strain components are defined: wrench simple shear; pure shear in XY (lateral stretch); and pure shear in YZ (vertical stretch). These biaxial strains can be viewed as the apices of a 'strain triangle' for unconfined transpression or transtension. The edges of the triangle correspond to: triaxial pure shear; non-coaxial, biaxial lateral extrusion; and the triaxial confined transpressional or transtensional strain of Sanderson and Marchini. During unconfined transpression, the orientation and, in particular, the geometry (k-value) of the finite-strain ellipsoid depends upon not only the amount of shortening across the zone and the amount of strike-slip parallel to the zone, but also upon the ratio of vertical to lateral stretch. This can present serious difficulties when attempting to use finite strains to infer the direction and magnitude of zone-boundary displacements.

Examples of transpression zones in which there is evidence of a component of lateral extrusion are described from SW Cyprus and central Scotland. These examples illustrate that antithetic strike-slip shearing is a kinematic requirement of laterally unconfined transpression, implying that synchronous shear-sense indicators may give opposite senses of movement in shear zones. Specific geometric and mechanical boundary conditions, together with internal fault-zone rheologies, may favour the lateral extrusion of material. Kinematic partitioning can occur to form fault-bounded domains in which end-member biaxial and/or non-coaxial strains are developed. Analysis of such domains can give a clearer understanding of regional-scale triaxial deformations. These findings illustrate the importance of establishing displacement boundary conditions when qualitatively or quantitatively analysing crustal deformation zones. © 1997 Elsevier Science Ltd.

INTRODUCTION

One consequence of plate kinematic theory is that, in addition to compressive, extensional and transcurrent displacements, plates moving over the surface of a sphere are likely to experience oblique relative motions, which Harland (1971) termed transpression and transtension. Harland's description, although mainly conceptual, discussed many of the geometric and kinematic consequences of oblique plate motion, and his insight has formed the basis for a large number of papers that have improved our understanding of deformation in three (and sometimes four) dimensions. Concepts discussed by Harland (1971) include the segmentation and partitioning of oblique plate boundaries into discrete deformational domains, lateral variations in structural style in different parts of an irregular plate margin, the inherent structural anisotropy and complexity arising from oblique collision, the consequences of non-coaxial incremental strain during crustal shortening, the change in structural style during progressive transpressional deformation and possible compatibility problems associated with lateral extrusion. We define lateral extrusion (also known as 'axial elongation' (Harland, 1971) or 'lateral escape' (Dias and Ribeiro, 1994)) as *a stretch in the horizontal direction that causes a deformation zone to lengthen (or shorten in transtension) relative to the undeformed rocks that comprise the zone margins.*

By imposing a number of well-defined boundary conditions that were not implicit in Harland's original concept, Sanderson and Marchini (1984) were able to derive an elegant and succinct mathematical model for transpression. Sanderson and Marchini specifically considered constant-volume homogeneous deformation in a vertical zone that was laterally confined and had a fixed basal surface, so that shortening across the zone was balanced entirely by vertical extrusion towards the upper free surface (Fig. 1a). Although such boundary conditions are unlikely to be fully realized in naturally occurring deformation zones, the idealized model of Sanderson and Marchini has been shown to be an

*Present address: Department of Earth Science, University of Liverpool, Liverpool L69 3BX, U.K.

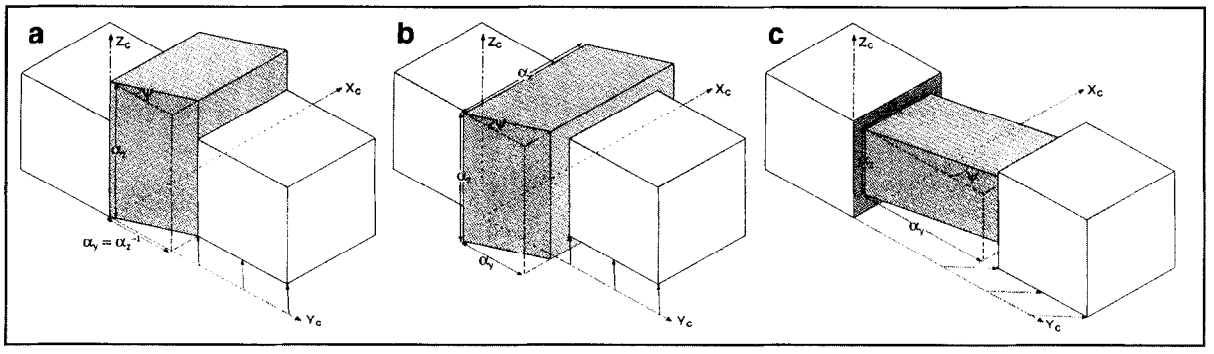

Fig. 1. Models of transpression–transtension showing the transformation of a unit cube assuming constant volume. (a) Transpression zone which is laterally and basally confined: horizontal shortening perpendicular to the zone, α_y, is balanced entirely by upward vertical thickening, α_z (based on Sanderson and Marchini, 1984, fig. 1). $\alpha_x = 1$. (b) Unconfined transpression zone: horizontal shortening across the zone is balanced both by upward and downward vertical thickening and by lateral extrusion. (c) Unconfined transtension zone: horizontal extension across the zone is balanced by vertical thinning and lateral shortening. The zones of deformation are shaded, the undeformed rocks on either side of the zones are unshaded. α_x, α_y and α_z are the stretches of the unit cube parallel to the Cartesian axes, X_c, Y_c and Z_c. For constant-volume deformation $\alpha_y = (\alpha_x \alpha_z)^{-1}$. ψ is the angular shear strain in the $X_c Y_c$ plane.

effective starting point when analysing three-dimensional deformation. In particular, by precluding the possibility of lateral stretch, their model avoids the lateral incompatibility (the 'space problem') that is generally assumed to be associated with axial elongation (e.g. Harland, 1971; pp. 36–38; Ramsay and Huber, 1987, pp. 610–613).

In this paper we extend the applicability of the mathematical description developed by Sanderson and Marchini (1984) by studying the importance of one of the main boundary conditions they introduced; we examine transpressional and transtensional strain in deformation zones that are not laterally or vertically confined, i.e. material can move into transtension zones or out of transpression zones parallel to the length of the zone, and the zone can thicken or thin vertically downwards as well as upwards towards the Earth's surface (Fig. 1b & c). By expanding the mathematical definition of transpression to incorporate the effects of lateral extrusion, we are able to present a more generalized model for describing three-dimensional non-coaxial deformation, and to provide a numerical and conceptual model for describing bulk deformation in crustal regions in which evidence for lateral extrusion has been observed in orogens and arcs (e.g. Harland, 1959, 1971; Tapponnier and Molnar, 1976; Molnar and Tapponnier, 1977; Dewey *et al.*, 1986; Avé Lallemant and Guth, 1990; McCaffrey, 1992). We then apply the model to examples of transpression zones in SW Cyprus and Scotland where there is field evidence that lateral extrusion has occurred.

THEORY

The strain matrix for finite transpressional strain

By choosing to define a set of Cartesian axes with orientations parallel and perpendicular to the shear-zone margins (Fig. 1a), Sanderson and Marchini (1984) developed a factorization scheme in which bulk finite transpressional deformation can be factorized into two separate plane-strain components, one a pure shear and the other a simple shear. This has proven to be conceptually useful as it allows complex non-coaxial three-dimensional strains to be visualized in terms already familiar to geologists accustomed to analysing plane-strain pure and simple shear.

In our analysis we follow Sanderson and Marchini (1984) in considering a deformation zone with vertical and parallel zone boundaries, bounded by undeformed blocks that experience relative displacement only in terms of non-rotational bulk translation in the horizontal plane (Fig. 1a). As a first-order approach, such boundary conditions probably represent a reasonable approximation to lithospheric plates undergoing oblique collision or extension. At this stage of the analysis we also retain the assumption that deformation is homogeneous and constant volume. Although this is generally geologically unrealistic, it helps to simplify the analysis conceptually, and the individual effects of each assumption can be analysed mathematically at a later stage. The main difference between our analysis and that of Sanderson and Marchini (1984), is that we remove the boundary restriction that specifies that the sides and base of the zone are confined (Fig. 1b & c).

In general terms a stretch, α, in a given direction is defined by:

$$\alpha = L\,L_o^{-1} = 1 + e = \sqrt{\lambda}$$

where L is the length of a passive marker after deformation, L_o is the original length of the marker prior to deformation, e is extension and λ is the quadratic extension (e.g. Ramsay, 1967). Positive values of e are extensional, negative values are contractional. We can enhance the model of Sanderson and Marchini (1984) to allow for a lateral stretch by replacing the

existing matrix describing the component of plane-strain pure shear with a non-plane-strain (i.e. triaxial) pure-shear matrix:

$$\begin{pmatrix} 1 & 0 & 0 \\ 0 & \alpha_z^{-1} & 0 \\ 0 & 0 & \alpha_z \end{pmatrix} \qquad \begin{pmatrix} \alpha_x & 0 & 0 \\ 0 & \alpha_y & 0 \\ 0 & 0 & \alpha_z \end{pmatrix}$$

plane-strain pure shear (constant volume) — non-plane-strain pure shear (constant volume)

where α_x, α_y and α_z are the principal stretches parallel to the Cartesian axes, X_c, Y_c and Z_c, respectively. α_x is the lateral stretch, and for constant volume $\alpha_y = (\alpha_x\alpha_z)^{-1}$. Figure 1(b) shows a transpression zone in which shortening across the zone is balanced by lateral extrusion together with vertical upward and vertical downward thickening; the factorized pure-shear *component* of the bulk deformation describes an oblate strain. Similarly, extension across a transtension zone is accommodated by vertical and lateral thinning (Fig. 1c), and the factorized strain ellipsoid for the pure-shear component is prolate.

The non-plane-strain pure-shear component can be further factorized into separate XY and YZ plane-strain components, which for constant volume are as follows:

$$\begin{pmatrix} \alpha_x & 0 & 0 \\ 0 & \alpha_y & 0 \\ 0 & 0 & \alpha_z \end{pmatrix} = \begin{pmatrix} \alpha_x & 0 & 0 \\ 0 & \alpha_x^{-1} & 0 \\ 0 & 0 & 1 \end{pmatrix} \begin{pmatrix} 1 & 0 & 0 \\ 0 & \alpha_z^{-1} & 0 \\ 0 & 0 & \alpha_z \end{pmatrix}.$$

non-plane-strain pure shear — plane-strain pure shear in XY — plane-strain pure shear in YZ

(1)

Applying this to equation (1) of Sanderson and Marchini (1984) gives a transpressional deformation, D:

$$D = \begin{pmatrix} 1 & \gamma & 0 \\ 0 & 1 & 0 \\ 0 & 0 & 1 \end{pmatrix} \begin{pmatrix} \alpha_x & 0 & 0 \\ 0 & \alpha_x^{-1} & 0 \\ 0 & 0 & 1 \end{pmatrix} \begin{pmatrix} 1 & 0 & 0 \\ 0 & \alpha_z^{-1} & 0 \\ 0 & 0 & \alpha_z \end{pmatrix}$$

simple shear — pure shear in XY (lateral stretch) — pure shear in YZ (vertical stretch)

$$= \begin{pmatrix} \alpha_x & \gamma(\alpha_x\alpha_z)^{-1} & 0 \\ 0 & (\alpha_x\alpha_z)^{-1} & 0 \\ 0 & 0 & \alpha_z \end{pmatrix}$$

unconfined transpression

(2)

where γ is the finite shear strain parallel to the zone such that $\gamma = \tan\psi$ (see Fig. 1).

The deformation matrix in equation (2) shows how general, unconfined, transpression can be expressed in terms of three separate plane-strain shear components. This is shown diagrammatically in Fig. 2, in which the apices of the deformation triangle represent the three individual plane-strain components, each of which is a biaxial end-member in a spectrum of three-dimensional deformation. The lower edge of the triangle represents triaxial pure shear (cf. Ramsay, 1967; Reches, 1978), whilst the right edge represents laterally confined transpression similar to that described by Sanderson and Marchini (1984). The left edge of the triangle represents a plane-strain deformation in which there is no vertical stretch ($\alpha_z = 1$), and all shortening across the deformation zone is balanced by lateral extrusion (Dias and Ribeiro, 1994). In this case, the overall deformation is no longer transpressional or transtensional in the restricted sense of Sanderson and Marchini (1984). However, the deformation, which remains non-coaxial and is still the result of oblique shortening, is clearly within the definition of transpression as used by Harland (1971), and this emphasizes that the definition of Sanderson and Marchini is not as broad as Harland's original concept.

The area inside the triangle covers all possible triaxial combinations of the three biaxial end-member strains, and represents all possible transpressional deformations described by equation (2). We propose that these deformations are referred to as *unconfined transpression*.

Finite transpressional strain ellipsoid

The shape and orientation of the finite-strain ellipsoid can be derived from the strain matrix in equation (2) for any given value of α_x, α_z and γ (see Appendix). Figures 3 and 4 present a number of plots that show the shape (Fig. 3) and orientation (Fig. 4) of the strain ellipsoid for a range of values of simple shear (γ) and orthogonal shortening (α_y), assuming constant volume deformation. The orthogonal shortening (α_y) in each plot differs in the ratio of lateral stretch (α_x) to vertical stretch (α_z), where $\alpha_y = (\alpha_x\alpha_z)^{-1}$. More strictly, this ratio, R_{LV}, is the amount of lateral extension, e_x, vs vertical extension, e_z:

$$R_{LV} = e_x/e_z.$$

Figure 3 shows that the boundary conditions that determine whether a deformation zone is *laterally* confined can have a profound effect upon the resultant strain in the zone. Note that removing the assumption that homogeneous deformation is *basally* confined does not change the geometry of bulk strain (see Discussion later).

Any measured finite-strain geometry resulting from laterally confined transpression can be considered in terms of a unique combination of pure-shear and simple-shear components (Fig. 3a) (Sanderson and Marchini, 1984, fig. 2). In contrast, Fig. 3(b–e) shows that by removing the assumption that a zone is laterally confined, we see that there is no longer a unique combination of strain components capable of causing a given shape of finite-strain ellipsoid, i.e. finite strain is now the result of *three* independent variables, pure shear, α_y, simple shear, γ, and the ratio of lateral to vertical extension, R_{LV}. Because field geologists studying finite strain also typically measure three variables (the orientation of the strain ellipsoid with respect to the shear-zone boundaries, θ', and two ratios of the

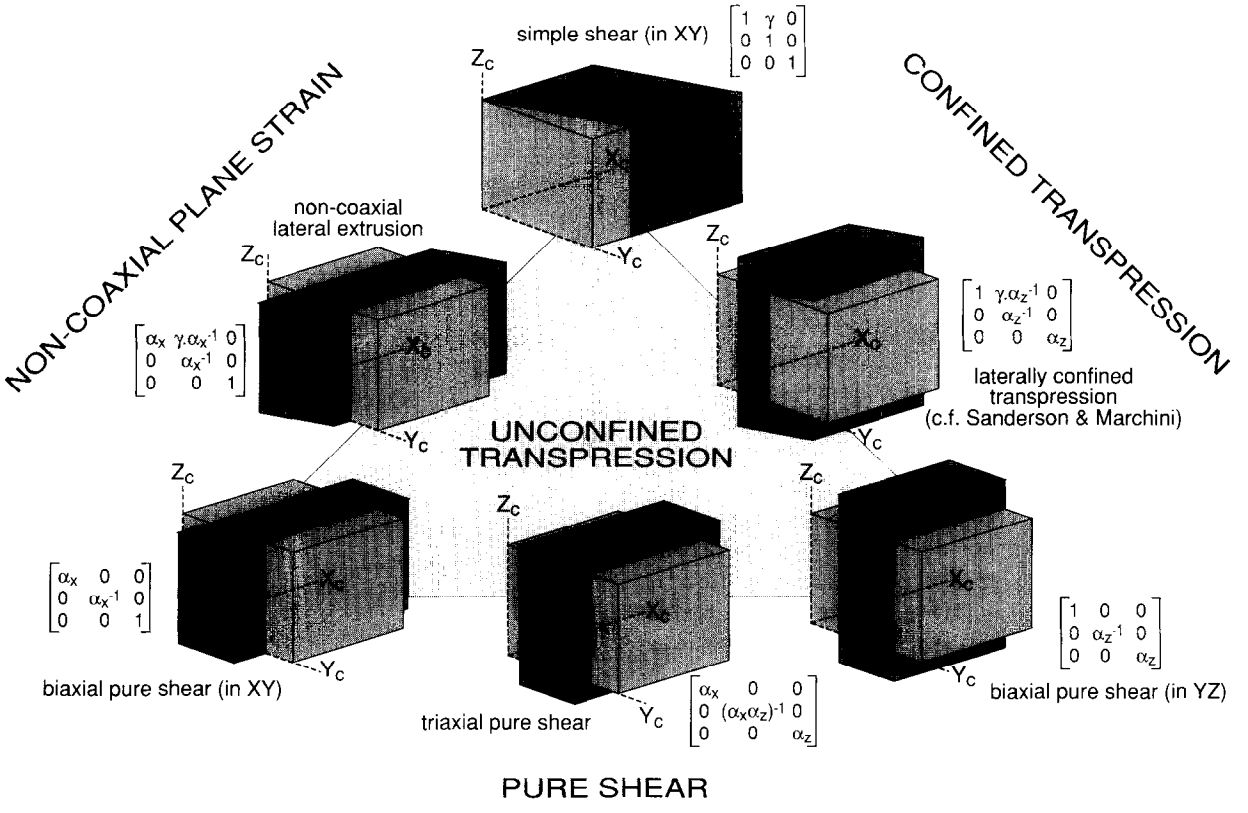

Fig. 2. Schematic diagram showing how unconfined transpression can be expressed in terms of three separate plane-strain components, represented by the three apices of the strain triangle. Each edge of the triangle represents a limited range of deformations between two end-member strain components. The interior of the triangle represents a full spectrum of homogeneous constant-volume transpressional deformation in which the boundary condition specifying lateral confinement has been removed.

length of principal axes of the strain ellipsoid, X_s:Y_s and Y_s:Z_s), it is theoretically possible that a unique solution could be derived using θ' that allows each strain component to be specified. In practice, however, the variation in ellipsoid orientation for different ratios of vertical to lateral stretch is very small (Fig. 4a–c), and will usually be completely masked by the statistical uncertainty of typical field measurements (see insets to Fig. 4). This has important implications for the application of mathematical transpression models to naturally occurring transpressional deformation; in general it will *not* even be possible to interpret homogeneous three-dimensional strain in terms of individual plane-strain factors, *unless* we can demonstrate unequivocally that no lateral extrusion has occurred, or unless we can quantify the amount of vertical and/or lateral stretch (or their ratio). This again emphasizes the necessity of studying the boundaries of deformation zones, in addition to deformation-zone interiors.

Incremental transpressional strain

Figures 3 and 4 represent only finite strains, and carry no implication of particular strain histories (i.e. the lines on the diagram do not represent deformation paths, a point emphasized by Sanderson and Marchini, 1984). Any given strain can be factorized in an infinite number of different ways. The factorization chosen by Sanderson and Marchini (1984) was mathematically convenient, as it allowed the component of finite shear strain to be expressed directly in terms of angular shear, γ (equation 2). Although their finite-strain matrix was formulated in terms of a pure shear followed by a simple shear, Sanderson and Marchini (1984, p. 451) also described how the matrix could be used to model incremental strain in an approximate way. A more rigorous approach was developed by Fossen and Tikoff (1993) and Tikoff and Fossen (1993), who derived a transpressional strain matrix expressed in terms of pure and simple shears acting simultaneously, allowing strain histories and deformation paths to be modelled more precisely. We can incorporate lateral extrusion into their strain matrix to derive the following matrix for unconfined homogeneous transpression resulting from simultaneous pure shearing and simple shearing:

$$D = \begin{pmatrix} \alpha_x & \Gamma_{xy} & 0 \\ 0 & (\alpha_x\alpha_z)^{-1} & 0 \\ 0 & 0 & \alpha_z \end{pmatrix} \quad (3)$$

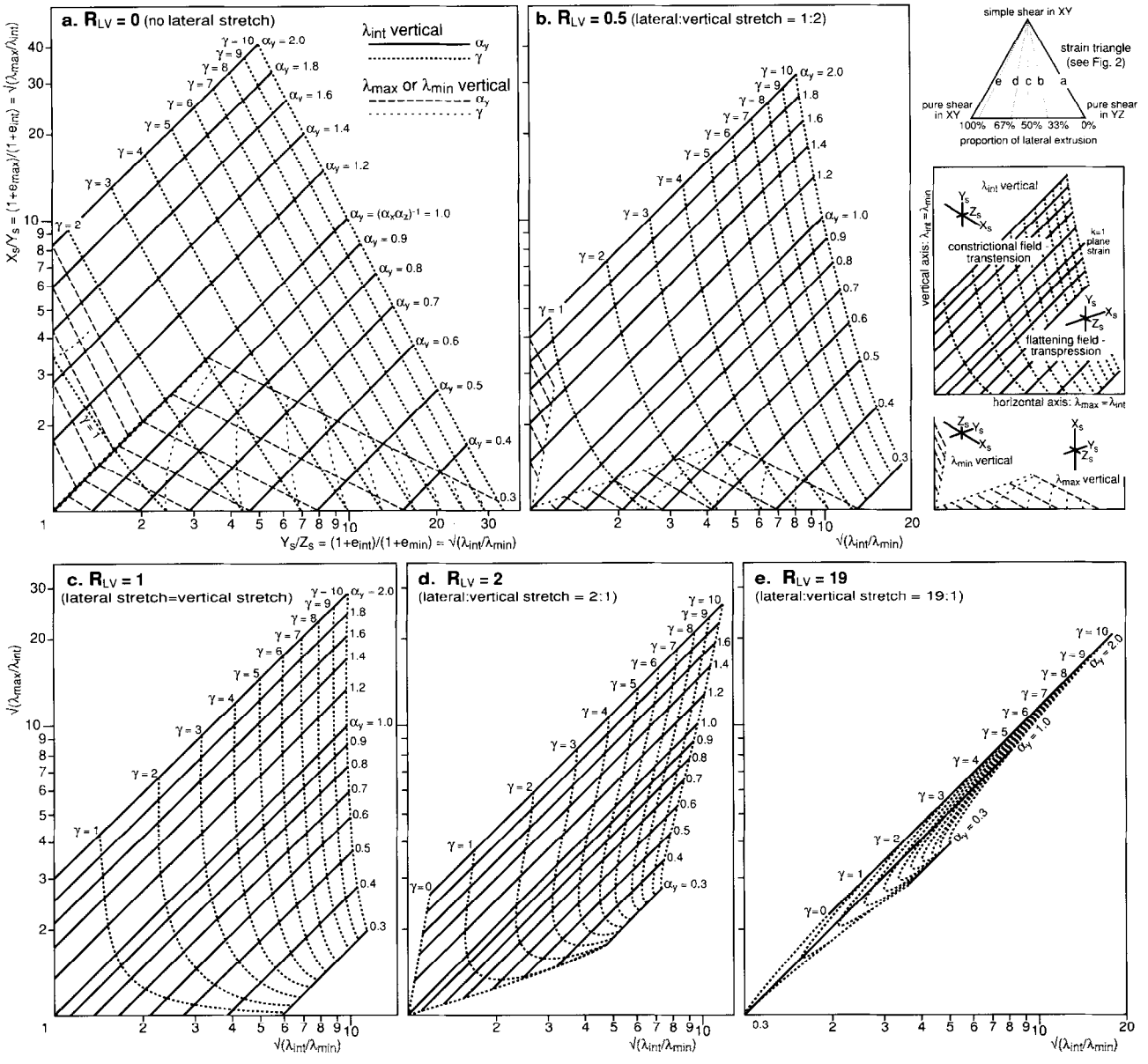

Fig. 3. Series of deformation plots (Flinn diagrams) showing the shape of the finite-strain ellipsoid, produced by constant-volume transpression and transtension, for a range of values of simple shear (γ) and orthogonal stretch (α_y). Each plot shows the possible strain geometries for a different ratio of lateral to vertical extension, R_{LV}, with (a) representing confined transpression (see Sanderson and Marchini, 1984, fig. 2), and (b)–(e) representing increasing proportions of lateral stretch. Deformation in which orthogonal shortening is balanced entirely by lateral extrusion is plane strain ($R_{LV} = \infty$), and all possible ellipsoid geometries lie on the '$k = 1$' diagonal of the Flinn plot. X_s, Y_s and Z_s are the principal axes of the finite-strain ellipsoid such that $X_s > Y_s > Z_s$. The marked variation in each of the graphs emphasizes that the amount of lateral stretch has a very significant effect on the resultant strain ellipsoid (and reciprocally, that strain geometries measured in the field cannot generally be interpreted in terms of any single pair of unique γ and α_y values). Uppermost inset diagram (top right) relates these plots to the transpression triangle in Fig. 2. Centre inset diagram shows how each plot consists of a constrictional field (transtension) and flattening field (transpression), separated by the $k = 1$ plane-strain diagonal. For transpression in which vertical stretch is more dominant than lateral extrusion (plots a and b), both the constrictional and flattening fields describe strain geometries in which the intermediate strain axis, Y_s, can be either vertical (centre inset diagram) or horizontal (lower inset diagram). Purely prolate strains (defined by the ordinate of the Flinn plot) and oblate strains (defined by the abscissa) cannot be represented when $R_{LV} > 1$ (plots d and e).

where the effective shear strain, $\Gamma_{xy} = \gamma_{FT}(\alpha_x - (\alpha_x\alpha_z)^{-1})/\ln(\alpha_x^2\alpha_z)$, and γ_{FT} is the shear strain for simultaneous pure and simple shearing (see Fossen and Tikoff, 1993). Because equations (2) and (3) are different, deformation and orientation plots based on the two equations will also differ in detail (compare fig. 2 of Sanderson and Marchini, 1984 with fig. 7 of Fossen and Tikoff, 1993). However, in general terms strain plots derived from equation (3) are very similar to Figs 3 and 4; the proportion of lateral shortening vs vertical thickening has a significant effect on the shape of the strain ellipsoid, but negligible effect on the ellipsoid orientation.

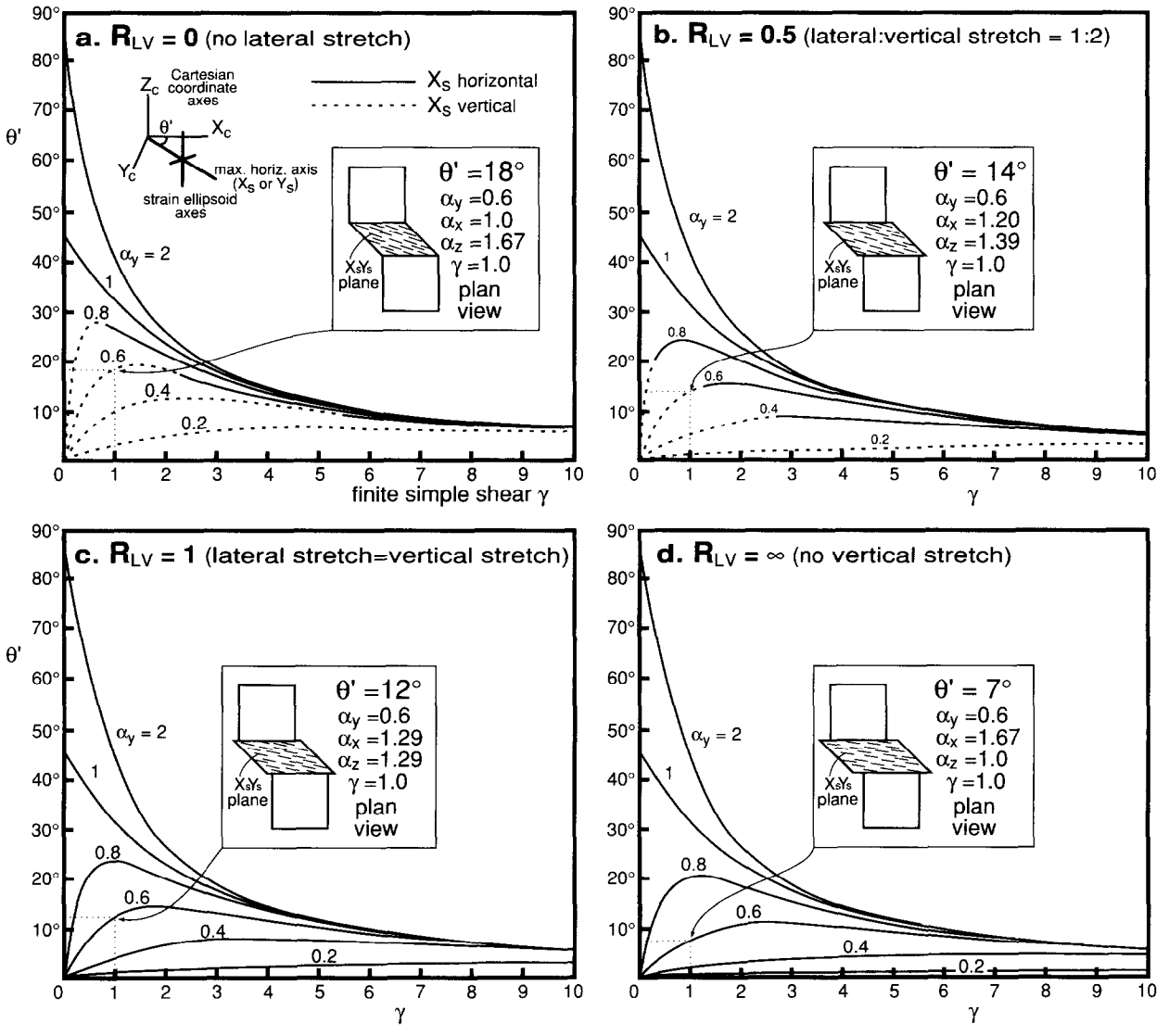

Fig. 4. Four plots showing the orientation of the longer axis of the finite-strain ellipsoid in the horizontal plane (θ') for a range of values of simple shear (γ) and orthogonal stretch (α_y). Each plot shows the possible strain geometries for a different ratio of lateral to vertical stretch. The similarity of the four diagrams emphasizes that the amount of lateral extrusion has little effect on ellipsoid orientation. This is also shown schematically in the inset diagrams which depict the orientation of the XY plane of the strain ellipsoid (cleavage?) for one particular transpressional boundary displacement. Only when vertical thickening dominates over lateral extrusion ($R_{LV} < 1$) in transpression (not transtension) can the short axis of the strain ellipsoid be vertical (plots a & b).

In general, it cannot be assumed that the ratio of lateral to vertical stretch will necessarily remain constant during progressive deformation. For individual deformation paths in which the R_{LV} ratio does vary, it is not possible to interpret all intermediate strain states with only one strain grid of the type shown in Fig. 3(a–e). Instead, a whole spectrum of strain grids is needed, covering a range of R_{LV} values.

Kinematic analysis

For simplicity, our analysis so far has followed Sanderson and Marchini (1984) in making the assumption that deformation is homogeneous. A consequence of this approach is that the deformation-zone boundaries in our model (Fig. 1b) have the unfeasible mechanical property of allowing free slip in all directions, whilst still transmitting the horizontal shear stress imparted by the component of horizontal simple shear (e.g. Ramsay and Huber, 1987, pp. 609–615; Schwerdtner, 1989; Robin and Cruden, 1994). Nevertheless, the advantage of assuming homogeneous strain is that the model is thereby able to express *bulk* deformation in terms of *generalized* strain parameters, allowing *qualitative* predictions about the kinematics of heterogeneous deformation to be made.

For example, by considering displacement vectors for points at the deformation-zone boundaries we are able to show the necessary kinematic displacements required to balance the strain geometrically across the zone (Fig. 5). For general transpressional and transtensional zones in

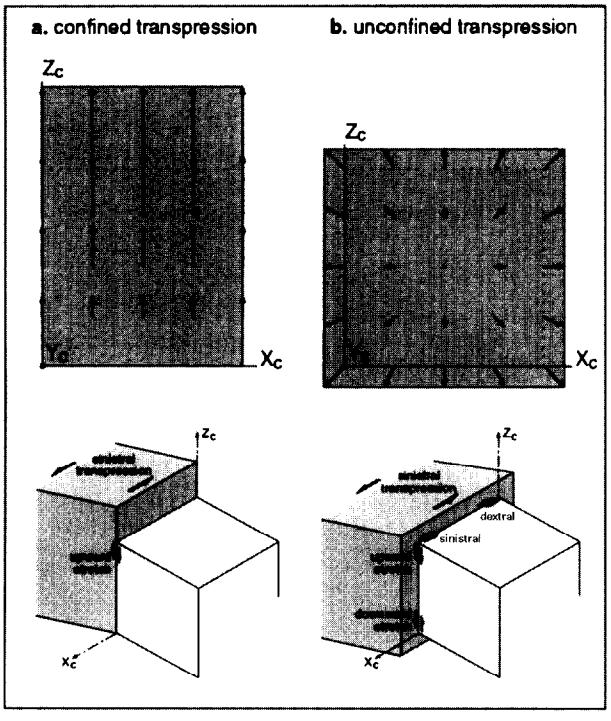

Fig. 5. Schematic displacement vectors for points lying along the deformation-zone boundary plane (i.e. the plane that contains the X_c and Z_c axes in Fig. 1). X_c, Y_c and Z_c are the Cartesian axes. The vectors show displacement paths for particles in the deformation zone immediately adjacent to the zone boundary, relative to immediately adjacent neighbouring particles on the opposite side of the zone boundary (i.e. on the undeformed zone margin). (a) Laterally and basally confined transpressional shortening balanced entirely by thickening vertically upwards (see Fig. 1a). Because the zone is basally confined, the deformation in this plane has a pin-line along the X_c axis. (b) Unconfined transpressional shortening balanced both by lateral extrusion, and thickening vertically upwards and downwards (see Fig. 1b). The deformation has a pin-point, which is shown here schematically at the centre of the zone-boundary plane, although the position may vary in actual transpression zones. The homogeneous deformation shown here is idealized, and requires zone boundaries that are mechanically unfeasible. Deformation in naturally occurring transpression zones is unlikely to be entirely restricted to the single planes of the zone boundaries, and the schematic displacements vectors shown here can be considered to represent the overall general tendency of distributed deformation.

which shortening is at least partially balanced by lateral stretch, as described by equations (2) and (3), there is a kinematic requirement that some material is displaced with an opposing sense of shear to the simple-shear deformation component acting across the whole zone. Similarly, zones in which the base is not confined require downwards displacements at depth for transpression, and upwards displacements at depth for transtension (see Discussion later). These displacement vectors should not be inferred to represent actual movement vectors in a single fault plane or shear zone; in reality there is an infinite number of ways in which strain can be accommodated in heterogeneous, geologically realistic situations. However, Fig. 5 emphasizes the inherent three-dimensional kinematic complexity that we must expect to find in naturally occurring transpression and transtension zones, and to show that apparent antithetic displacements in transpression zones need not necessarily be explained in terms of separate phases of deformation with opposing senses of shear.

Strain partitioning during unconfined transpression

During oblique transpressional shortening there is a marked tendency for individual pure-shear and simple-shear strain components to be spatially partitioned into separate deformational domains (e.g. Oldow *et al.*, 1990; Molnar, 1992; Fossen *et al.*, 1994; Tikoff and Teyssier, 1994; Teyssier *et al.*, 1995; Jones and Tanner, 1995; see also Jiang and White, 1995). In particular, a non-coaxial strain component is often partially or wholly partitioned into discrete narrow zones dominated by simple-shear wrenching, which delineate broader zones of distributed, largely co-axial, deformation (i.e. pure shear). Molnar (1992) argued that partitioning can occur during transpression because oblique slip faults are often inherently unstable (McKenzie and Jackson, 1983). Tikoff and Teyssier (1994) showed that partitioning might occur because of the non-coaxiality of instantaneous strains during progressive transpressional deformation. The arguments developed by Tikoff and Teyssier (1994) are important, and emphasize the significance of analysing progressive deformation, as well as boundary conditions, when studying transpression.

As with confined transpression zones, strain partitioning in laterally *unconfined* zones may cause the preferential factorization of the non-coaxial component into narrow zones of simple shear, but, unlike confined zones, the remaining coaxial shear component can be distributed across a wider zone of *triaxial* pure shear (e.g. central Scotland; see below). This type of strain partitioning can be considered with reference to Fig. 2, where bulk transpressional strain is now expressed by two separate domains, one situated near the top of the transpressional triangle (simple shear), the other towards the base of the triangle (triaxial pure shear), with a horizontal position determined by the ratio of vertical to lateral stretch (cf. inset to Fig. 9). In brittle regimes, triaxial deformation can be manifested as three or four sets of oblique faults, each with oblique displacement vectors (Reches, 1978, 1983; Reches and Dietrich, 1983).

Alternatively, it is possible for transpressional deformation to be partitioned into broad domains of non-coaxial plane strain in the horizontal X_cY_c plane, together with localized, narrow domains of biaxial pure shear in the vertical Y_cZ_c plane. This is a possible interpretation for Late Mesozoic deformation in SW Cyprus, as discussed below. These conceptual models show that the manifestation of unconfined transpression can be very complex in naturally occurring shear zones, and that strain may be partitioned into several different types of deformational domain, including any of the three biaxial end-member strains shown at the apices of the strain triangle (Fig. 2), or conceivably, domains

represented by any position on the edges or anywhere inside the triangle. Furthermore, some domains during progressive deformation might be active only for short periods, whilst others may change deformational style over time; i.e. deformation is commonly non-steady (Jiang and White, 1995), and partitioning of strain can be temporal as well as spatial.

As emphasized by Fig. 4, it can be very difficult in practice to interpret *homogeneous* non-coaxial triaxial (i.e. 'unconfined') bulk transpression. However, some of these practical difficulties are resolved when bulk strain has been strongly partitioned, so that domains are described by points lying on the apices (or left or bottom edges) of the strain triangle shown in Fig. 2 (e.g. Scotland, see below). This is because in such situations, strain within some domains might be triaxial *or* non-coaxial, but not both (and it is the combination of the two components that gives rise to complications in interpretation at outcrop scale). Interpretation of overall *bulk* partitioned strain (i.e. interpretation of far-field displacements) remains complex, and requires domain boundaries and relationships between neighbouring domains to be analysed in detail. Interpretation is particularly complicated when strain has been compartmentalized into disparate domains at several different scales.

EXAMPLES OF LATERAL EXTRUSION IN TRANSPRESSION ZONES

Examples of deformation involving lateral extrusion have been proposed in orthogonal collision zones such as Eastern China and Tibet (Molnar and Tapponnier, 1977), Eastern Anatolia (Dewey *et al.*, 1986) and Central Asia (Cobbold and Davy, 1988). In most cases, it has been suggested that the regional pure shear was accommodated along conjugate strike-slip faults or shear-zone arrays that facilitate lateral escape of crustal blocks, particularly during the collision of irregularly shaped continental margins (McKenzie, 1972; Dewey and Burke, 1973) or late in an orogenic cycle in overthickened plateau regions (England and McKenzie, 1982; Dewey *et al.*, 1986).

Along-strike extension or compression can occur in arc regions that are situated along transpressional subduction margins where the obliquity of convergence varies, either due to the plate margin being curved or to the presence of a nearby pole of relative plate rotation (e.g. McCaffrey, 1992, fig. 5). Possible examples of along-strike extension (i.e. lateral extrusion) have been documented in Sumatra (McCaffrey, 1991) and the Aleutians (Ekström and Engdahl, 1989). Arc-parallel extension may act as an important mechanism in the exhumation of high-pressure–low-temperature metamorphic rocks in accretionary wedges (e.g. the Cretaceous plate margin of Venezuela; Avé Lallemant and Guth, 1990).

Lateral extrusion in ancient transpression zones has generally not been considered, although Gilotti and Hull (1993) discussed a model for deformation in the Scandinavian Caledonides in which regional shortening along décollements gave rise to extension parallel to orogenic strike, synchronous with sinistral strike-slip. Dias and Ribeiro (1994) introduced the concept of lateral extrusion during transpression as one of several ways to explain the complex finite-strain patterns observed in the Ibero-Amorican arc. Recent detailed kinematic analysis of a Mesozoic dextral strike-slip duplex in New Jersey (Laney and Gates, 1996) has shown that, internally, fault-bound horses have undergone vertical, horizontal and oblique movements. These displacements are attributed by the authors to 'extrusional shuffling' within a restraining bend region that accommodates shortening of the duplex normal to the bounding faults.

Here, we outline two examples of regional transpression zones in which there is qualitative field evidence for lateral extrusion during transpression. In both cases, it is suggested that lateral extrusion has occurred due to specific boundary conditions imposed upon the deformation zones.

The Troodos–Mamonia suture zone, SW Cyprus

In SW Cyprus, serpentinite-filled fault zones mark the tectonic suture between two oceanic complexes: the Upper Cretaceous Troodos complex and the Triassic–Lower Cretaceous Mamonia complex (Fig. 6). The suture zone can be subdivided into two segments that display significantly different deformational characteristics: a northern area dominated by well-documented, top-to-the-west thrust tectonics (Lapierre, 1975; Malpas *et al.*, 1993); and a southern area where E–W-trending, anastomosing, subvertical, serpentinite-filled fault zones preserve evidence of both strike-slip (Swarbrick, 1993) and compressional motions (Malpas *et al.*, 1993). In this paper we are concerned with the faults and associated serpentinites in the southern area (Fig. 6).

A chronology of deformation, metamorphism and hydration has been deduced from field and laboratory studies (optical and SEM analysis) of structures and deformation textures in the serpentinite-filled fault zones of the southern area. High-temperature (approximately 800–925°C) mylonitic peridotite fabrics are preserved in less altered, relict blocks of mantle material within the serpentinites, and display dextral kinematic indicators (asymmetric and offset porphyroclasts). These are thought to have formed early in the deformation history, possibly during displacements along an E–W-trending oceanic transform fault that penetrated mantle material (cf. the nearby Arakapas Fault Zone; inset Fig. 6; MacLeod and Murton, 1993). The dextral fabrics clearly pre-date the sinistral transpressional deformation we discuss below, and are not considered here further.

Subsequent hydration of the mantle rocks to form serpentinite led to their density-driven uprise and intrusion along the fault zones, a process possibly triggered by the substantial volume increases associated with serpen-

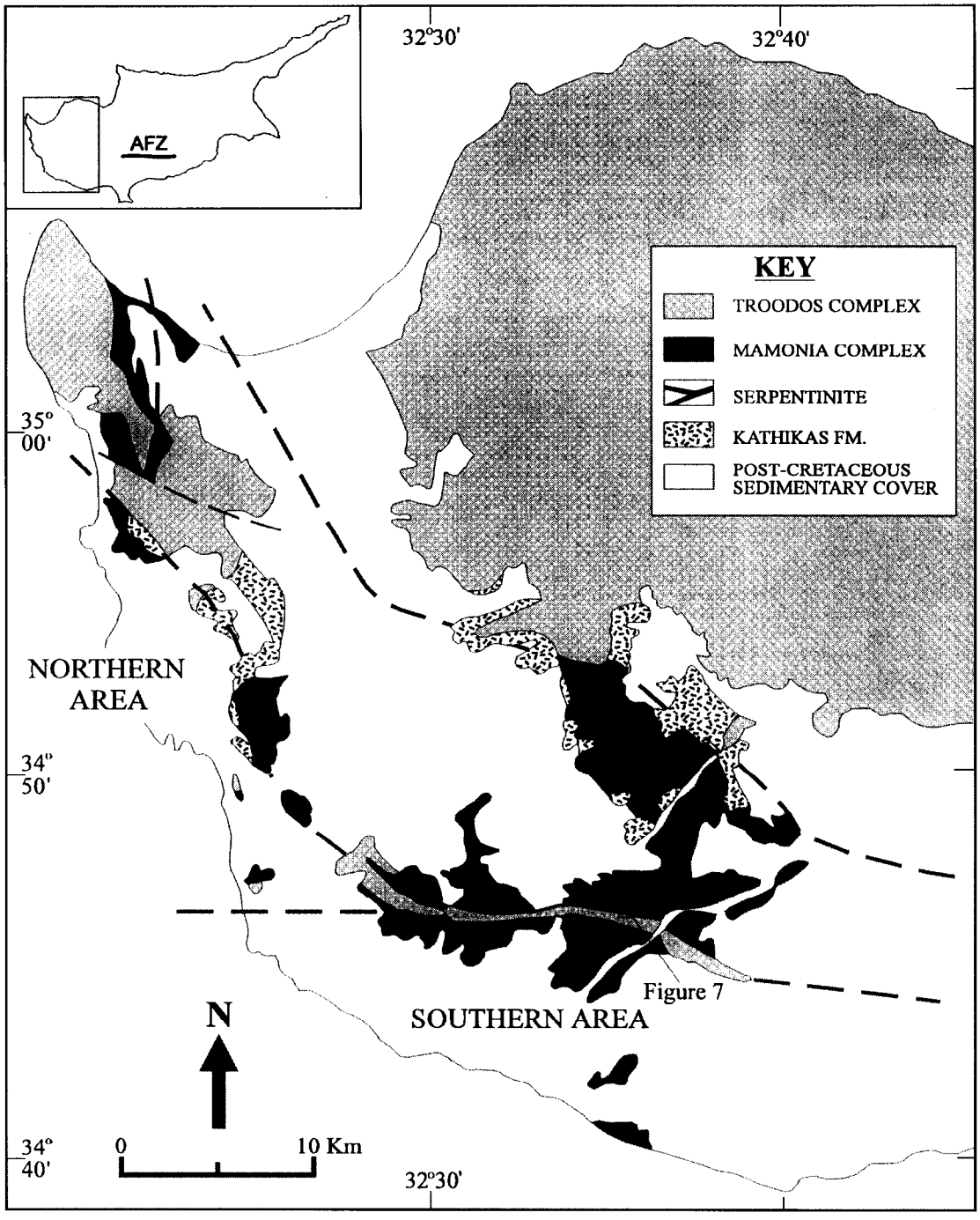

Fig. 6. Regional map of SW Cyprus showing the location of the detailed map shown in Fig. 7. AFZ is the Arakapas Fault Zone.

tinization reactions (25–45%; Coleman, 1971; O'Hanley, 1992). This hydration was followed by a regional phase of sinistral transpression thought to be associated with the final docking of the Troodos and Mamonia complexes (Swarbrick, 1993). The widespread occurrence of lizardite shows that the later deformation occurred at significantly lower temperatures (e.g. the upper stability limit of lizardite at 3 kbar is less than 500°C according to Bowen and Tuttle, 1949, or less than 350°C according to Coleman, 1971). $^{18}O/^{16}O$ studies from comparable serpentinites in the Troodos Massif indicate temperatures in the region of 100°C (Margaritz and Taylor, 1974).

The later sinistral transpression produced complex arrays of anastomosing faults and shear zones that appear to be preferentially developed in the zones of ultrabasic material that had previously undergone the greatest amounts of serpentinization during mantle hydration. A representative structural dataset from one of the E–W-trending fault zones is shown in Fig. 7.

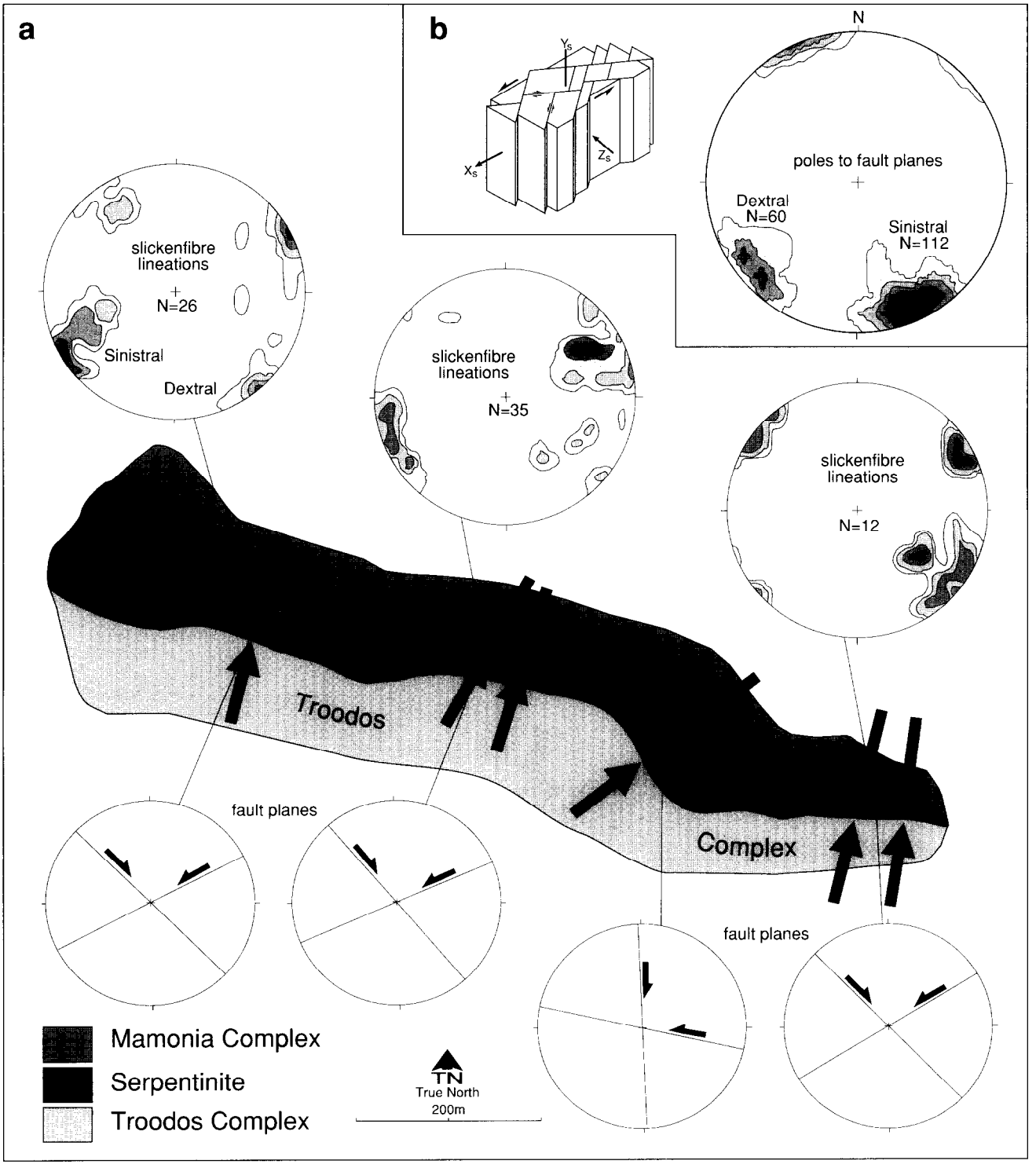

Fig. 7. (a) Simplified geology of a fault zone in the Mamonia area, with stereonets showing slickenfibre lineations and summary fault planes. (b) Representative stereonet of poles to fault planes showing that the short axis of the strain ellipsoid is contained in the obtuse angle between conjugate faults. Complex and irregular slickenfibre measurements from serpentinite 'lozenges' have been omitted in order to exclude the effects of small-scale block rotations.

Although it is not possible to quantify the magnitude of strain, bulk deformation is interpreted to be transpressive based on the following observations.

(1) the serpentinites are enclosed within subvertical, fault-bounded belts (Swarbrick, 1993). Low-temperature deformation is accommodated by steeply dipping shear zones displaying macroscopically ductile cataclastic flow and brittle fault arrays. As both shear zones and faults are kinematically identical, they are interpreted as being broadly coeval (Bailey, 1997).

(2) The faults and shear zones form an anastomosing

network of mutually cross-cutting (i.e. conjugate) structures that enclose lenticular lozenges of less-deformed and serpentinized material on all scales.

(3) Faults and shear zones preserve numerous lineations defined by serpentine mineral slickenfibres. In higher-strain regions, the majority of lineations are subhorizontal to shallowly plunging (Fig. 7), and associated kinematic indicators preserve predominantly strike-slip senses of shear. They include asymmetric extensional shear bands, *S–C* fabrics, offset clasts, minor fold vergence and Reidel-type shears. Sinistral kinematic indicators are up to twice as predominant as dextral. The marginal regions and interiors of low-strain lozenges often display complex and variable orientations of slickenfibres. These formed due to the rotation and internal distortion of the lozenges within the higher-strain matrix of the serpentinite belts and are thought to be of little regional significance; they are therefore omitted from the lineation data shown in Fig. 7.

(4) The lizardite-dominated serpentinites are semi-ductile, as the obtuse (rather than acute) angle between conjugate sets contains the axis of principal compression (Fig. 7) (see also Ramsay and Huber, 1987, fig. 26.29). In most locations, the compression axis bisecting conjugate arrays lies a few degrees clockwise of being orthogonal to the local zone boundaries. This is consistent with high-angle oblique sinistral shortening (i.e. pure-shear-dominated sinistral transpression).

(5) Locally, the boundaries of the serpentinite zones are defined by moderately to shallowly dipping, top-to-the-southwest and, more rarely, top-to-the-northeast overthrusts with associated oblique or dip-slip slickenfibres. This represents a local partitioning of the pure-shear deformation, in which minor amounts of horizontal shortening are accommodated by vertical thickening manifested as thrust stacking.

(6) There is no field evidence to indicate that large-scale partitioning of strike-slip displacements onto certain major fault strands has occurred.

Consequently, although the paucity of adequate strain markers precludes a *complete* description of the regional finite-strain ellipsoid, the geometry and kinematics of the conjugate faults and shear zones show that the dominant direction of elongation of the strain ellipsoid was axial to the zone rather than vertical. In existing transpression models this observation is broadly incompatible with transpressional deformation that is demonstrably dominated by pure shear (Tikoff and Teyssier, 1994; Teyssier *et al.*, 1995). In confined transpression, as modelled by Sanderson and Marchini (1984) and Fossen and Tikoff (1993), the finite extension direction for pure-shear-dominated transpression is vertical (whether or not strain partitioning, as modelled by Tikoff and Teyssier, 1994, has occurred). This is not necessarily the case for unconfined transpression, and the field data from SW Cyprus are consistent with our model for unconfined transpression in which lateral extrusion has occurred.

Three related features of the serpentinite-filled fault zones may explain why material was extruded laterally in this case. First, the pre-existing serpentinite-filled suture zone may have possessed an irregular geometry that included lateral free surfaces, so that NNE–SSW shortening would have lead to the lateral movement of material along the length of the fault zone. Such architecture can be inherited from pre-existing complex fault-zone geometries that include numerous promontories and embayments (cf. Harland, 1971; McKenzie, 1972; Dewey and Burke, 1973), although there is little evidence to suggest that this was an important factor in SW Cyprus. More significantly, irregular zone geometries can result from the non-uniform distribution of irregular serpentinite intrusions in some parts of the fault zone and not others. Isolated serpentinite bodies are well documented along many oceanic fracture zones (e.g. Bonatti and Crane, 1984), forearcs (e.g. Keen *et al.*, 1989) and mid-ocean ridge-parallel highs (e.g. Bonatti, 1976). Several small intrusive units of serpentinite that were not significantly affected by later deformation are preserved in SW Cyprus (e.g. Vatomandra, Nea Kholetria), and all display highly irregular geometries.

A second possibility is that the upward mobility of the serpentinite (giving rise to vertical thickening) may have been hindered by a large amount of overburden or the presence of a strong 'cap rock'. This process is seen on a small scale in the Ayia Varvara area, where an isolated serpentinite intrusion has 'mushroomed' against an overlying Troodos lava 'roof', suggesting that vertical ascent has been prevented.

Third, in laboratory deformation experiments lizardite serpentinites have been shown to be demonstrably weak when compared to most other rocks, and tend to deform in a ductile manner by stable sliding (Dengo and Logan, 1981; Gates and Kambin, 1990). The widespread preservation of fibrous serpentine and carbonate minerals, in the form of slickenfibres along dilatant shear fractures and in numerous vein arrays, also implies the existence of high pore fluid pressures at the time of deformation, and this may have led to further weakening. Such a low-strength material would be relatively mobile in comparison to the wall rocks, and would therefore be easily able to move laterally along faults during imposed deformation.

The development of thrusts along some serpentinite belt margins may also be determined by local boundary conditions. Pre-existing, shallowly dipping contacts are locally preserved adjacent to these thrusts and appear to have formed during earlier serpentinite protrusion (Bailey, 1997). In these areas, horizontal shortening may have been more easily accommodated by thrust-sense reactivation of the pre-existing, shallowly inclined contacts.

Our overall interpretation is that particular boundary conditions were imposed on the deformation of the serpentinites leading to unconfined transpression in the serpentinite-filled suture zones of SW Cyprus. These

conditions may arise from the pre-existing protrusive geometry of the serpentinites, their weak rheology during subsequent deformation and restrictions imposed on their upwards displacement by overlying strata.

Mid-Devonian upper crustal deformation in central Scotland

In mid-Devonian times the Neoproterozoic and Palaeozoic rocks of central Scotland experienced a widespread low-magnitude deformation that involved open folding and subsequent fracturing. The timing of deformation is constrained by the unconformable deposition of Upper Old Red Sandstone (ORS) sediments over the denuded fold limbs of pervasively fractured Lower ORS strata.

A first-order model based upon the interpretation of the geometry and kinematics of mesofractures in central Scotland (see Jones and Tanner, 1995) suggests that regional shortening was orientated approximately N–S, oblique (i.e. sinistrally transpressive) to the pre-existing ENE–WSW Highland Boundary Fault Zone ('HBFZ'). The HBFZ is interpreted to have reactivated as a structurally weak zone of marked anisotropy that strongly influenced deformation in central Scotland, causing the regional partitioning of transpressional strain into a narrow domain of mainly non-coaxial plane strain along the HBFZ, balanced by wider domains of predominantly coaxial shear flanking the zone. However, this model is an over-simplification in several ways. First, the transpressional strain has not been completely partitioned between the first-order deformational domains. Second, the strain within each of the domains is not distributed homogeneously, and evidence of second-order strain partitioning can be observed. Third, the model assumes that no lateral extrusion has occurred, and this is now considered in more detail.

Rocks south of the HBFZ have been shortened by the low-amplitude, long-wavelength, upright Strathmore and Sidlaw folds (Fig. 8). This asymmetric fold pair represents an overall bulk shortening of approximately 10–15%, with highest strains found closest to the HBFZ. The parallelism of the fold axes with the HBFZ is evidence of regional strain partitioning (Jones and Tanner, 1995), and the folds define a domain of coaxial shear strain in which horizontal shortening across the deformation zone caused the domain to thicken *vertically*. In the late stages of deformation, brittle failure occurred on a regional scale, and rocks on both sides of the HBFZ were transected by arrays of discrete fractures.

Figure 8 shows the interpretation of a mesofracture study in central Scotland (following the methodology outlined by Hancock, 1985). The amount of brittle fracturing is high in a small number of sampling stations, all of which lie very close to the HBFZ (Ramsay, 1964; Jones, 1990). Such sites display a conjugate set of vertical fractures in which sinistral faults are often much more numerous and have larger displacements than dextral faults; strain is biaxial and non-coaxial (the sinistral and dextral faults represent Riedel and conjugate Riedel shears respectively; cf. Wilcox *et al.*, 1973), and the intermediate principal strain axis is vertical and neutral (e.g. Fig. 8a). The faulting at such sites represents the rotation and elongation of the finite-strain ellipse in the horizontal plane.

In mesofracture sampling sites situated further from the HBFZ, brittle strain is much lower than the high-strain sites flanking the fault. Mesofractures are steeply dipping (but not vertical), and usually form four mutually intersecting coeval fracture sets (e.g. Fig. 8b & c), indicating that strain is triaxial rather than biaxial (Oertel, 1965; Reches, 1978, 1983; Aydin and Reches, 1982; Reches and Dietrich, 1983; Hancock, 1985; Krantz, 1988). In such cases strain is irrotational, and the intermediate principal axis of the strain ellipsoid is vertical and has undergone extension (i.e. strains are oblate), allowing us to infer that lateral stretch was much more dominant than vertical stretch during the fracturing phase. Clearly, this contrasts with the strain represented by the Strathmore and Sidlaw folds, which represent significant vertical stretch but negligible lateral extrusion (Fig. 9). Such a switch in the orientation of principal strain axes might imply a change in the orientation of the far-field stress system through time, or may simply be represent a difference between finite strain (recorded by folding) and a late-stage increment of infinitesimal strain recorded by fracturing (Tikoff and Teyssier, 1994; C. Teyssier, personal communication). It is also possible that the strong anisotropy of lithified Lower ORS red-bed strata allowed lateral stresses to be stored elastically during folding, until the elastic strength of the rock was finally exceeded and brittle failure occurred (i.e. that there was temporal strain partitioning, as well as spatial strain partitioning).

In summary, because the simple-shear component of regional transpression was partitioned into the HBFZ, the domains flanking the HBFZ are dominated by pure shear, and the irrotational strain in the pure-shear domains is easier to analyse and less ambiguous to interpret than domains containing non-coaxial deformation. In the pure-shear domains we can demonstrate that strain represented by brittle fracturing is triaxial, with a maximum extensional strain that is horizontal and orientated broadly parallel to the transpression-zone boundaries. It is important to emphasize that in terms of bulk strain, the amount of vertical stretch accomplished by Strathmore–Sidlaw folding (up to 10%) is much greater than the amount of lateral extrusion represented by faulting (less than 5%). Nevertheless, the mesofracture analysis shows that a component of lateral extrusion (with respect to the HBFZ) did occur in central Scotland in mid-Devonian times.

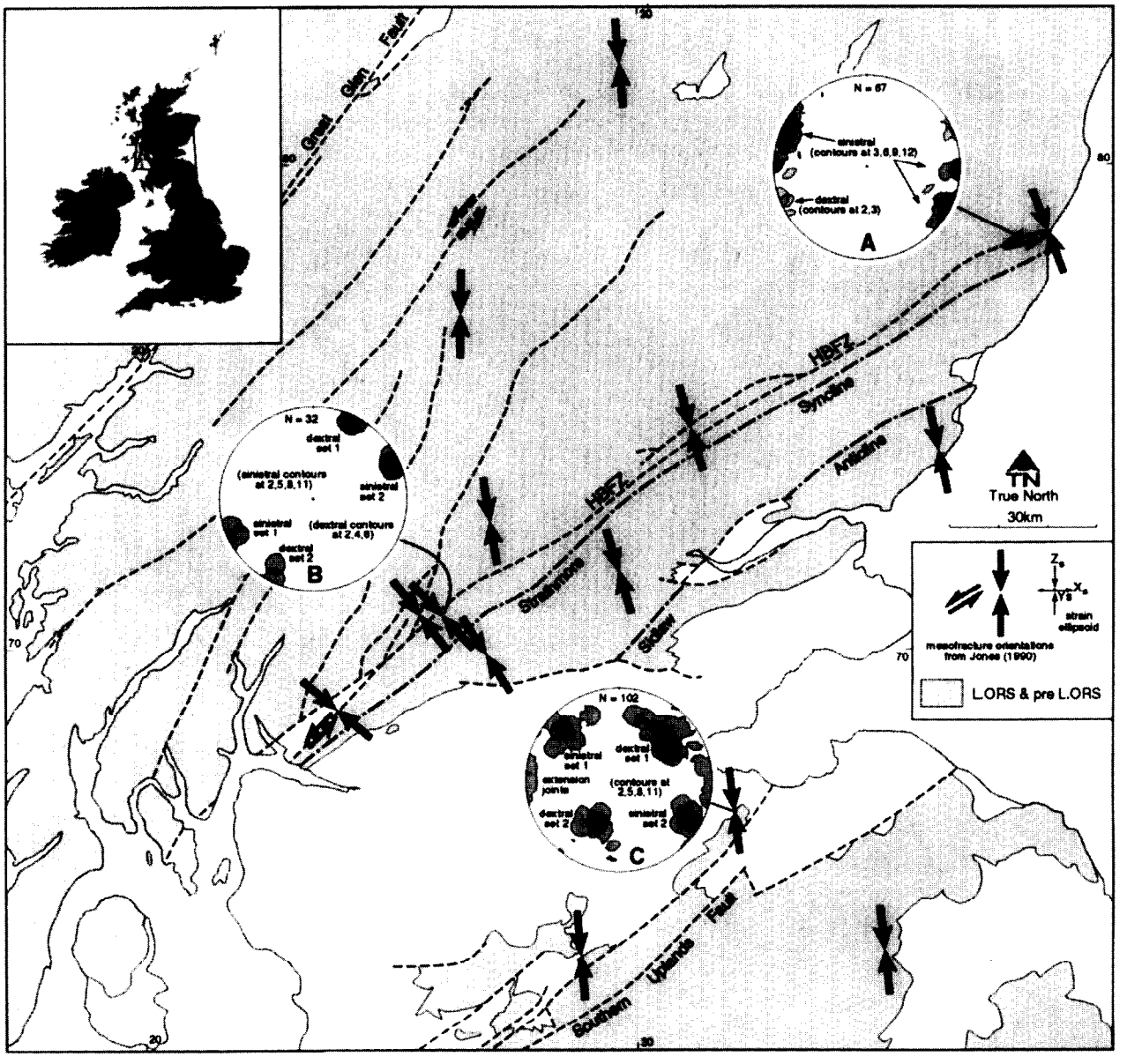

Fig. 8. Interpretation of a mesofracture analysis of mid-Devonian deformation in central Scotland. The Strathmore syncline and Sidlaw anticline south of the Highland Boundary Fault Zone (HBFZ) represent upper-crustal regional shortening and vertical thickening of the Lower ORS strata. Inset stereonets show representative fracture patterns: (a) high brittle strain adjacent to the HBFZ dominated by sinistral faults representing Riedel shears; (b) uncommonly low-strain domain close to the HBFZ showing triaxial fracture patterns (fractures are visibly non-vertical and demonstrably represent four discrete fracture sets); and (c) triaxial fracture patterns in which abundance and magnitude of sinistral and dextral faults are approximately equal. See text for further details.

DISCUSSION

Using finite strain to interpret zone-boundary displacements

The mathematical model we have presented for unconfined transpression involves the standard (Lagrangian) approach used in strain modelling, i.e. deformation is applied to the undeformed state under specified boundary conditions, and the resultant strain is analysed. Most analyses of naturally occurring shear zones rely on the inverse (Eulerian) approach of using finite strain to infer zone-boundary displacement (e.g. Shackleton and Ries, 1984) and/or boundary conditions (e.g. our studies of strain in SW Cyprus and central Scotland). However, our consideration of unconfined transpression, particularly the orientation of the strain ellipsoid presented in Fig. 4, shows the potential danger of making untested assumptions about boundary conditions when using finite strain to infer the directions of zone-boundary displacement. Consequently, geometric constructions for interpreting transpression zones, such as those developed

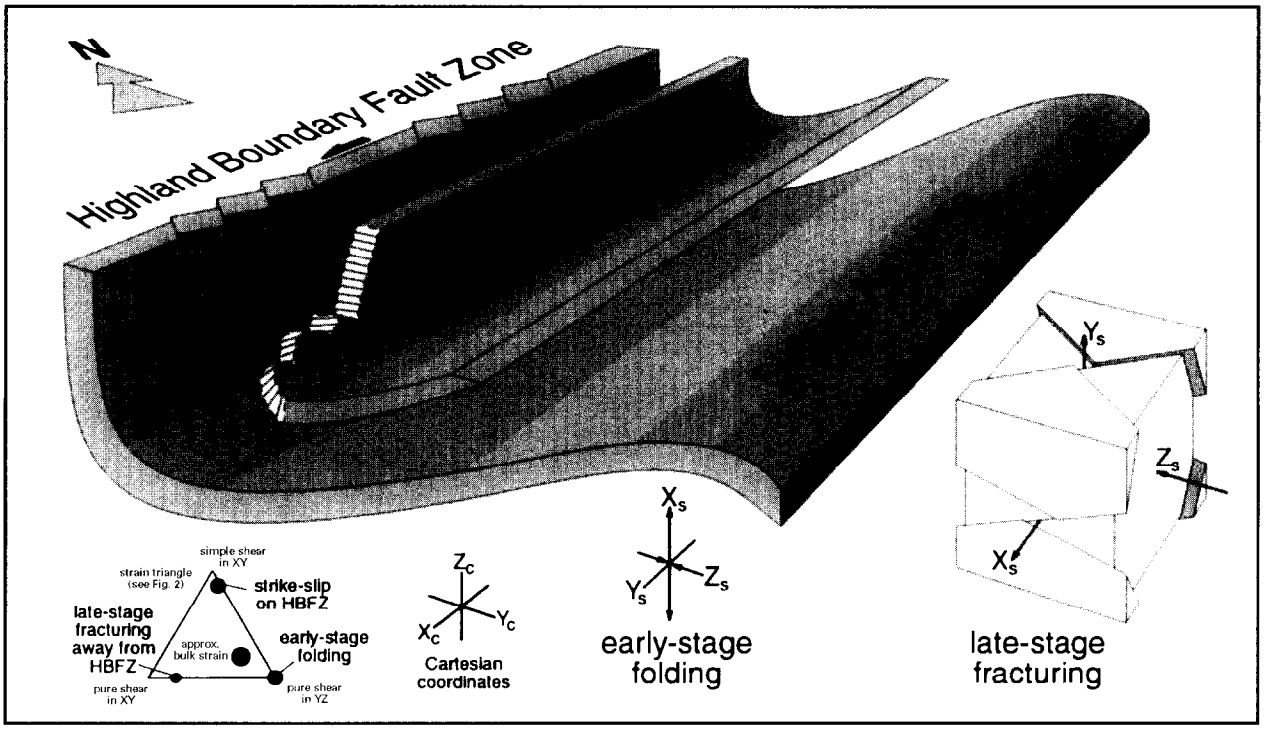

Fig. 9. Schematic diagram showing an interpretation of mid-Devonian deformation in central Scotland, south of the Highland Boundary Fault Zone (HBFZ), and the difference in the attitude of the principal axes of the strain ellipsoid between early-stage folding and late-stage fracturing.

by McCoss (1986), should not be used unless lateral extrusion is shown not to have occurred (as stated very clearly by McCoss, 1986, p. 718). In practice, however, because the orientation of the finite-strain ellipsoid is not strongly dependent upon the ratio of vertical to lateral stretch, the construction may still often give an approximately correct result (typically $\pm 10°$ or better), even though the underlying method is no longer rigorous.

These complications, together with those introduced when strain is partitioned (Jones and Tanner, 1995, p. 801), or when strain is the result of non-steady flow (Jiang and White, 1995), show that the relationship between finite strain at the outcrop scale and the boundary conditions imposed by regional plate motions is potentially extremely complex.

Basally unconfined transpression

During homogeneous transpression the shape of the finite-strain ellipsoid is not dependent upon the boundary condition that specifies whether the deformation is *basally* confined (in contrast, removing the boundary condition that confines the transpression zone *laterally* does have a very significant effect on the shape of the strain ellipsoid, as shown in Fig. 3). In other words, basal confinement does not affect the bulk strain geometry within an idealized homogeneous zone, but rather the way in which the strain is vertically distributed through the crust with respect to an external reference frame, i.e. the undeformed blocks flanking the zone (compare Fig. 1a with the right edge of the deformation triangle in Fig. 2). Transpression models incorporating basally unconfined deformation allow stretch to occur vertically downwards, as well as at the upper free surface (see Sanderson and Marchini, 1984, fig. 13), and are probably more representative of naturally occurring crustal-scale transpression and transtension zones.

In basally unconfined transpression we can define a horizontal plane which can be considered as a neutral 'pin-level' (in some ways analogous to the 'pin line' used in cross-section balancing), defining points that are experiencing no relative vertical displacement with reference to the undeformed blocks flanking the zone (Fig. 5). Points above and below the plane are displaced away from the plane during transpression, or towards the plane during transtension. Upper crustal transpression zones, such as SW Cyprus and central Scotland, lie above the pin-level because of the close proximity of the upper free surface, and are dominated by compressional structures. In basally confined zones the neutral plane is, by definition, the base of the zone.

Modelling heterogeneous transpression

It is possible to model individual shear zones more completely by removing the assumption that deformation is homogeneous, and replacing specific terms in the transpression strain matrix (equation 2 or equation 3)

with more complex functions (typically sinusoidal or parabolic). This allows a component of strain to vary in magnitude across the shear zone, which more closely matches naturally occurring deformation zones in which strain typically decreases gradually from the centre of the zone towards the unstrained zone margins (e.g. Ramsay and Huber, 1987, pp. 610–613; Robin and Cruden, 1994). It is possible to model heterogeneous lateral extrusion in this way by adding a specific 'y-dependent' function to the lateral stretch component; $\alpha_x = f(y)$, and/or to model heterogeneous vertical stretch in a similar way, $\alpha_z = f(y)$.

Such refinements to the strain matrix do help to create a mathematical model that overcomes some of the mechanical difficulties that arise when homogeneous deformation is assumed (Ramsay and Huber, 1987, pp. 609–613; Schwerdtner, 1989), and can make interesting predictions about geometry and kinematics in transpression zones. The disadvantage of this type of analysis is that whilst these *ad-hoc* models add realism, they usually also add significant mathematical complexity, and can often actually reduce the accessibility and applicability of the model and its ability to describe bulk deformation in terms of generalized, simplified strain components.

An additional problem concerning strain heterogeneity in general, is that in naturally occurring deformation zones the concept of heterogeneity is usually scale-dependent. Although the strain *within* an individual shear zone can be modelled, as described, by a single matrix with 'y-dependent' pure- and simple-shear terms, on larger (and smaller) scales of observation the distribution of strain is often heterogeneous in a much less regular way; strain is concentrated into narrow shear zones that form the boundaries of wide domains of low strain, or is partitioned into individual domains between which the style of deformation differs considerably (e.g. Cobbold, 1977; Bell, 1981; Lister and Williams, 1983).

Free surfaces—why does lateral extrusion occur?

Models for laterally and basally confined transpression are conceptually convenient as they assume that all deformation is accomplished by distortion of the upper free surface. However, more realistic models must allow for the basal stretch that accompanies lithospheric thickening during orogenesis. Similarly, actual tectonic settings, in which irregularly shaped lithospheric plates interact with one another on the surface of a sphere, must generally also involve horizontal inter- and intra-plate forces that can induce or permit lateral stretch to occur. In this respect, neither the basal lithosphere–asthenosphere boundary, nor the lateral boundaries between adjacent plates are 'free' surfaces in an absolute sense; nevertheless, the upper free surface is not the only surface capable of distortion. Plates are in motion with respect to one another, their boundaries are deformable, and this can allow significant deformation, including lateral extrusion, to occur. Lateral extrusion was much more dominant than vertical thickening in the Mesozoic deformation in SW Cyprus. In contrast, lateral extrusion, although occurring to a minor extent, was of less significance in mid-Devonian deformation in central Scotland.

CONCLUSIONS

A mathematical description of 'unconfined' transpression (and transtension), in which the boundary conditions specified by Sanderson and Marchini (1984) have been extended to allow for lateral extrusion, is more representative of the original transpressional concept as defined by Harland (1971). Application of the mathematical model for unconfined transpression allows us to make the following conclusions.

(1) Constant-volume, homogeneous unconfined transpression and transtension, which in general are non-coaxial triaxial strains, can be considered in terms of a 'strain triangle' in which the three apices of the triangle represent three biaxial 'end-member' deformations. Confined transpression and transtension (Sanderson and Marchini, 1984) are described by one edge of the strain triangle.

(2) The shape and orientation of the finite-strain ellipsoid resulting from laterally unconfined transpression is dependent not only upon the amount of shortening across the zone and the amount of strike-slip parallel to the zone, but also upon the amount of lateral extrusion compared with vertical thickening, expressed as R_{LV}, the ratio of lateral to vertical extension. This ratio has a marked effect on the shape of the finite-strain ellipsoid, but a much lesser effect on its orientation in the horizontal plane, and this implies very significant practical difficulties when attempting to use finite strain to infer the direction and magnitude of zone-boundary displacements.

(3) For homogeneous deformation, bulk strain within the transpression zone is the same in basally confined and unconfined zones. It is probably more geometrically realistic to assume that crustal-scale transpression and transtension zones do thicken and thin vertically downwards and upwards, respectively.

(4) Antithetic strike-slip shearing is a kinematic requirement of laterally unconfined transpression and transtension zones, and need not imply a separate deformational event with an opposing sense of shear.

(5) Strain partitioning in unconfined transpression zones can occur in a variety of ways, so that individual deformational domains can be described by any point in the strain triangle. The practical difficulties of analysing non-coaxial triaxial strain (i.e. unconfined transpression) at the outcrop scale can be significantly reduced when the bulk strain has been partitioned into individual domains displaying only biaxial and/or non-coaxial strains, although interpretation remains complex on a regional scale and requires analysis of the boundary conditions of

each deformational domain. Strain partitioning can occur temporally as well as spatially.

(6) Late Mesozoic oblique compression in SW Cyprus caused pure-shear-dominated transpression in which shortening was largely accommodated by lateral extrusion, with only minor amounts of vertical stretch. In contrast, mid-Devonian pure-shear-dominated transpression in central Scotland was accommodated largely by vertical thickening, with only minor amounts of lateral extrusion.

(7) This study demonstrates that the displacement boundary conditions play an important part in controlling the local strain and displacement fields (cf. Smith, 1993).

Acknowledgements—The authors thank Geoff Tanner and colleagues at Glasgow University, Durham University, Østfold Research Foundation (STØ) and Tectonic Studies Group for previous discussions. The paper was improved considerably with the help of pertinent reviews by Christian Teyssier and Alexander Cruden. Stereonet software was written by Richard Allmendinger (Fig. 7) and Colin Farrow (Fig. 8). R. R. Jones and W. Bailey were financed by NERC studentships held at Glasgow and Durham universities, respectively. Additional funding for R. R. Jones was provided by STØ through a grant from NORAS, and for R. E. Holdsworth by the Department of Geological Sciences, University of Durham.

REFERENCES

Avé Lallemant, H. G. and Guth, L. R. (1990) Role of extensional tectonics in exhumation of eclogites and blueschists in an oblique subduction setting, northwest Venezuela. *Geology* **18**, 950–953.

Aydin, A. and Reches, Z. (1982) Number and orientations of fault sets in the field and in experiments. *Geology* **10**, 110–112.

Bailey, W. R. (1997) The structural evolution of a microplate suture zone, SW Cyprus. Unpublished Ph.D. thesis, University of Durham.

Bell, T. H. (1981) Foliation development: the contribution, geometry and significance of progressive bulk inhomogeneous shortening. *Tectonophysics* **75**, 273–296.

Bonatti, E. (1976) Serpentinite protrusions in the oceanic crust. *Earth and Planetary Science Letters* **32**, 107–113.

Bonatti, E. and Crane, K. (1984) Oceanic fracture zones. *Scientific American* **250**(5), 36–47.

Bowen, N. L. and Tuttle, O. F. (1949) The system MgO–SiO_2–H_2O. *Bulletin of the Geological Society of America* **60**, 439–460.

Cobbold, P. R. (1977) Description and origin of banded structures. I. Regional strain, local perturbations, and deformation bands. *Canadian Journal of Earth Sciences* **14**, 1721–1731.

Cobbold, P. R. and Davy, P. (1988) Indentation tectonics in nature and experiment 2: Central Asia. *Bulletin of the Geological Institute, University of Uppsala* **14**, 143–162.

Coleman, R. G. (1971) Petrologic and geophysical nature of serpentinites. *Bulletin of the Geological Society of America* **82**, 918–987.

Dengo, C. A. and Logan, J. M. (1981) Implications of the mechanical and frictional behaviour of serpentinite to seismogenic faulting. *Journal of Geophysical Research* **86**, 10771–10782.

Dewey, J. F. and Burke, K. C. A. (1973) Tibetan, Variscan and Precambrian basement reactivation: products of continental collision. *Journal of Geology* **18**, 683–692.

Dewey, J. F., Hempton, M. R., Kidd, W. S. F., Saroglu, F. and Sengor, A. M. C. (1986) Shortening of continental lithosphere: the neotectonics of Eastern Anatolia—a young collision zone. In *Collision Tectonics*, eds M. P. Coward and A. C. Ries, pp. 3–36. Geological Society of London Special Publication **19**.

Dias, R. and Ribeiro, A. (1994) Constriction in a transpressive regime: an example in the Iberian branch of the Ibero-Armorican arc. *Journal of Structural Geology* **16**, 1543–1554.

Ekström, G. and Engdahl, E. R. (1989) Earthquake source parameters and stress distribution in the Adak Island region of the central Aleutian Islands, Alaska. *Journal of Geophysical Research* **94**, 15499–15519.

England, P. C. and McKenzie, D. P. (1982) A thin viscous sheet model for continental deformation. *Geophysical Journal of the Royal Astronomical Society* **70**, 295–321.

Fossen, H. and Tikoff, B. (1993) The deformation matrix for simultaneous simple shearing, pure shearing and volume change, and its application to transpression–transtension tectonics. *Journal of Structural Geology* **15**, 413–422.

Fossen, H., Tikoff, B. and Teyssier, C. (1994) Strain modelling of transpressional and transtensional deformation. *Norsk Geologisk Tidsskrift* **74**, 134–145.

Gates, A. E. and Kambin, R. C. (1990) Comparison of the natural deformation of the State-Line Serpentinite. U.S.A., with experimental studies. *Tectonophysics* **182**, 249–258.

Gilotti, J. A. and Hull, J. M. (1993) Kinematic stratification in the hinterland of the central Scandinavian Caledonides. *Journal of Structural Geology* **15**, 629–646.

Hancock, P. L. (1985) Brittle microtectonics: principles and practice. *Journal of Structural Geology* 7, 437–457.

Harland, W. B. (1959) The Caledonian sequence in Ny Friesland. Spitzbergen. *Quarterly Journal of the Geological Society of London* **114**, 307–342.

Harland, W. B. (1971) Tectonic transpression in Caledonian Spitzbergen. *Geological Magazine* **108**, 27–42.

Jiang, D. and White, J. C. (1995) Kinematics of rock flow and the interpretation of geological structures, with particular reference to shear zones. *Journal of Structural Geology* **17**, 1249–1265.

Jones, R. R. (1990) The mode and timing of microplate docking along the Highland Boundary Fault Zone, Scotland. Unpublished Ph.D. thesis, University of Glasgow.

Jones, R. R. and Tanner, P. W. G. (1995) Strain partitioning in transpression zones. *Journal of Structural Geology* **17**, 793–802.

Keen, M. J., Salisbury, M., Burke, M. and Ishii, T. (1989) Serpentinite seamounts of Pacific fore-arcs drilled by the Ocean Drilling Program: Dr Hess would be pleased. *Geoscience Canada* **16**(3), 177–182.

Krantz, R. W. (1988) Multiple fault sets and three-dimensional strain: theory and application. *Journal of Structural Geology* **10**, 225–237.

Laney, S. E. and Gates, A. E. (1996) Three-dimensional shuffling of horses in a strike-slip duplex: an example from the Lambertville sill, New Jersey. *Tectonophysics* **258**, 53–70.

Lapierre, H. (1975) Les formations sédimentaires et éruptives des nappes de Mamonia et leurs relations avec le massif de Troodos (Chypre occidentale). *Mémoires de la Société géologique de France, Paris* **123**, 420.

Lister, G. S. and Williams, P. F. (1983) The partitioning of deformation in flowing rock masses. *Tectonophysics* **92**, 1–33.

MacLeod, C. J. and Murton, B. J. (1993) Structure and tectonic evolution of the Southern Troodos Transform Fault Zone, Cyprus. In *Magmatism and Plate Tectonics*, eds H. M. Prichard, T. Alabaster, N. B. W. Harris and C. R. Neary, pp. 141–176. Geological Society of London Special Publication **76**.

Malpas, J., Calon, T. and Squires, G. (1993) The development of a late Cretaceous microplate suture zone in SW Cyprus. In *Magmatism and Plate Tectonics*, eds H. M. Prichard, T. Alabaster, N. B. W. Harris and C. R. Neary, pp. 177–195. Geological Society of London Special Publication **76**.

Margaritz, M. and Taylor, H. P. (1974) Oxygen and hydrogen isotope studies of serpentinization in the Troodos ophiolite complex, Cyprus. *Earth and Planetary Science Letters* **23**, 8–14.

McCaffrey, R. (1991) Slip vectors and stretching of the Sumatran forearc. *Geology* **19**, 881–884.

McCaffrey, R. (1992) Oblique plate convergence, slip vectors, and forearc deformation. *Journal of Geophysical Research* **97**, 8905–8915.

McKenzie, D. P. (1972) Active tectonics of Mediterranean region. *Geophysical Journal* **18**, 1–32.

McKenzie, D. P. and Jackson, J. (1983) The relationship between strain rates, crustal thickening, palaeomagnetism, finite strain and fault movements within a deforming zone. *Earth and Planetary Science Letters* **65**, 182–202.

McCoss, A. M. (1986) Simple constructions for deformation in transpression/transtension zones. *Journal of Structural Geology* **8**, 715–718.

Molnar, P. (1992) Brace–Goetze strength profiles, the partitioning of strike-slip and thrust faulting at zones of oblique convergence, and the stress–heat flow paradox of the San Andreas Fault. In *Fault Mechanics and Transport Properties of Rocks*, eds B. Evans and T.-F. Wong, pp. 435–459. Academic Press, London.

Molnar, P. and Tapponnier, P. (1977) Relation of the tectonics of eastern China to the India–Eurasia collision: application of slip line field theory to large-scale continental tectonics. *Geology* **5**, 212–216.
Oertel, G. (1965) The mechanism of faulting in clay experiments. *Tectonophysics* **2**, 343–393.
O'Hanley, D. S. (1992) Solution to the volume problem in serpentinisation. *Geology* **20**, 705–708.
Oldow, J. S., Bally, A. W. and Avé Lallement, H. G. (1990) Transpression, orogenic float, and lithospheric balance. *Geology* **18**, 991–994.
Ramsay, D. M. (1964) Deformation of pebbles in Lower Old Red Sandstone conglomerates adjacent to the Highland Boundary Fault. *Geological Magazine* **101**, 228–248.
Ramsay, J. G. (1967) *Folding and Fracturing of Rocks*. McGraw-Hill, New York.
Ramsay, J. G. and Huber, M. I. (1987) *The Techniques of Modern Structural Geology. Volume 2: Folds and Fractures*. Academic Press, London.
Reches, Z. (1978) Analysis of faulting in three-dimensional strain field. *Tectonophysics* **47**, 109–129.
Reches, Z. (1983) Faulting of rocks in three-dimensional strain fields. II. Theoretical analysis. *Tectonophysics* **95**, 133–156.
Reches, Z. and Dietrich, J. H. (1983) Faulting of rocks in three-dimensional strain fields. I. Failure of rocks in polyaxial, servo-controlled experiments. *Tectonophysics* **95**, 111–132.
Robin, P.-Y. F. and Cruden, A. R. (1994) Strain and vorticity patterns in ideally ductile transpression zones. *Journal of Structural Geology* **16**, 447–466.
Sanderson, D. J. and Marchini, W. R. D. (1984) Transpression. *Journal of Structural Geology* **6**, 449–458.
Schwerdtner, W. M. (1989) The solid-body tilt of deformed palaeohorizontal planes: application to an Archean transpression zone, southern Canadian Shield. *Journal of Structural Geology* **11**, 1021–1027.
Shackleton, R. M. and Ries, A. C. (1984) The relation between regionally consistent stretching lineations and plate motions. *Journal of Structural Geology* **6**, 111–117.
Smith, J. V. (1993) Kinematics of secondary synthetic ("P") faults in wrench systems. *Tectonophysics* **223**, 439–443.
Swarbrick, R. E. (1993) Sinistral strike-slip and transpressional tectonics in an ancient oceanic setting: the Mamonia Complex, southwest Cyprus. *Journal of the Geological Society of London* **150**, 381–392.
Tapponnier, P. and Molnar, P. (1976) Slip-line field theory and large-scale continental tectonics. *Nature* **264**, 319–321.
Teyssier, C., Tikoff, B. and Markley, M. (1995) Oblique plate motion and continental tectonics. *Geology* **23**, 447–450.
Tikoff, B. and Fossen, H. (1993) Simultaneous pure and simple shear: the unifying deformation matrix. *Tectonophysics* **217**, 267–283.
Tikoff, B. and Teyssier, C. (1994) Strain modelling of displacement-field partitioning in transpressional orogens. *Journal of Structural Geology* **16**, 1575–1588.
Wilcox, R. E., Harding, T. P. and Seely, D. R. (1973) Basic wrench tectonics. *Bulletin of the American Association of Petroleum Geologists* **57**, 74–96.

APPENDIX

$$\text{Fingertensor} = D.D^{\mathrm{T}} = \begin{pmatrix} (\alpha_x^4\alpha_z^2 + \gamma^2)(\alpha_x\alpha_z)^{-2} & \gamma(\alpha_x\alpha_z)^{-2} & 0 \\ \gamma(\alpha_x\alpha_z)^{-2} & (\alpha_x\alpha_z)^{-2} & 0 \\ 0 & 0 & \alpha_z^2 \end{pmatrix} \tag{A1}$$

where D is the strain matrix for unconfined transpression (equation 2). The eigenvalues of the Finger tensor are:

$$\begin{aligned} \lambda_1 &= (2^{-1}(\alpha_x\alpha_z)^{-2}(\gamma^2 + 1 + \alpha_x^4\alpha_z^2 + (\gamma^4 + 2\gamma^2 + 2\alpha_x^4\alpha_z^2\gamma^2 + 1 \\ &\quad - 2\alpha_x^4\alpha_z^2 + \alpha_x^8\alpha_z^4)^{1/2})) \\ \lambda_2 &= (2^{-1}(\alpha_x\alpha_z)^{-2}(\gamma^2 + 1 + \alpha_x^4\alpha_z^2 - (\gamma^4 + 2\gamma^2 + 2\alpha_x^4\alpha_z^2\gamma^2 + 1 \\ &\quad - 2\alpha_x^4\alpha_z^2 + \alpha_x^8\alpha_z^4)^{1/2})) \\ \lambda_3 &= \alpha_z^2 \end{aligned} \tag{A2}$$

$$\text{and the eigenvectors} = \begin{pmatrix} (\lambda_1\alpha_x^2\alpha_z^2 - 1)\gamma^{-1} & (\lambda_2\alpha_x^2\alpha_z^2 - 1)\gamma^{-1} & 0 \\ 1 & 1 & 0 \\ 0 & 0 & 1 \end{pmatrix} \tag{A3}$$